PEO Penetration into Water-Plasticized Poly(vinylphenol) Thin Films

Chen Lu,[†,⊥] Robert Richardson,[‡] Robert Pelton,[*,†] Terence Cosgrove,[§] and Kari Dalnoki-Veress[||]

McMaster Centre for Pulp and Paper Research, Department of Chemical Engineering, McMaster University, Hamilton, ONT, Canada L8S 4L7, H. H. Wills Physics Laboratory, University of Bristol, Tyndall Avenue, Bristol, BS8 1TL U.K., School of Chemistry, University of Bristol, Tyndall Avenue, Bristol, BS8 1TS U.K., and Department of Physics and Astronomy, McMaster University, Hamilton, ONT, Canada L8S 4L7

Received August 4, 2003; Revised Manuscript Received October 29, 2003

ABSTRACT: Neutron reflectivity was used to characterize the adsorption of poly(ethylene oxide) (PEO), 150 kDa, on both polystyrene (PS) and poly(vinylphenol) (PVPh), thin films in water. The PVPh films had thicknesses of 434 and 438 Å and contained 9% v/v water in contrast to the 492 Å PS film which contained no water. PEO did not adsorb on the PS film, while the specific adsorption of PEO on the PVPh film was 1.2 mg/m^2 at pH = 6.6. Reflectivity profiles from both deuterated and hydrogenated PEO in D_2O provided a comprehensive picture of PEO on/in the PVPh film. The PEO distribution was modeled by two uniform layers. The external layer was a 30 Å thick corona of PEO (12.5%v/v) in water. Between the corona and bulk PVPh film was a 25 Å interpenetration layer consisting of 22% PEO, 76% PVPh, and 2% water. Since the interpenetration layer accounted for 45% of the bound PEO, it is proposed that about half of each adsorbed PEO molecule enters the PVPh film. Thus, the PEO interaction with a PVPh hydrogel can be considered as an example of a polymer/polymer complex formation leading to nanoscale PEO/PVPh blend coated with a water-swollen PEO corona.

Introduction

The interaction of water-soluble polymers with surfaces is a fundamental aspect of many biological and industrial processes. Blood clot formation, biofilm generation, colloidal flocculation, and contact lens fouling all start with the interaction of an aqueous macromolecule with a surface. Fundamentally different types of surfaces can interact with aqueous polymers. At one extreme, surfaces such as silica or polyethylene can be smooth, nonporous and have a solid substrate containing no water. After initial contact with such an impenetrable surface, the adsorbed polymer may collapse and spread to give loops, trains, and tails. The properties of adsorbed polymers on such surfaces have been extensively studied both experimentally and theoretically.[1] At the other extreme are water-swollen hydrogel surfaces where soluble polymers may or may not bind. Nonbinding polymers, which are small relative to the gel mesh size, can diffuse into and through the gel.

In this paper, we describe an unusual case of polymer adsorption in which the adsorbing polymer is soluble in the solid substrate. Our surface is a spin cast film of poly(vinylphenol), PVPh, which contains about 10% v/v water. The adsorbing polymer is poly(ethylene oxide), PEO, which is known to have a strong attractive interaction with PVPh. Indeed, mixtures of pure PEO and PVPh form miscible blends.[2] This is an interesting system, because after initial contact the PEO can enter the PVPh film in addition to the normal spreading and collapse. In addition to being scientifically interesting, the formation of PEO embedded in surfaces may provide an alternative strategy to grafting and to block copolymer adsorption for preparation of PEO-rich surfaces for biocompatible materials.[3]

Neutron reflectivity measurements are sensitive to nanostructural features of the interfacial layers.[4,5] In this work, we use neutron reflectivity to characterize PEO adsorption onto and penetration into PVPh films. It will be shown that upon adsorption about half of the PEO molecule enters the PVPh film.

Experimental Section

Materials. Polystyrene (MW = 10 000 Da), poly(*p*-vinylphenol) (MW = 10 000 Da), and deuterated poly(ethylene oxide) (MW = 150 000 Da) were obtained from Polymer Source and used without further purification. Poly(ethylene oxide) Polyox N-80 (MW = 200 000 Da) was obtained from Union Carbide. P type boron-doped silicon wafers with diameters of 100 ± 0.5 mm, thicknesses 10 ± 0.1 mm, orientations 100, resistivities <0.1 Ω/cm, and both sides polished were purchased from ELCAT Inc. The silicon wafers were first cleaned by immersion in the mixture of sulfuric acid and H_2O_2 (30%, v/v) with volume ratio of 7:3. Afterward, they were rinsed with sufficient water and treated with a buffered 1 wt % HF aqueous solution (7:1 NH_4F/HF) for 3 min. The HF treatment removed the surface oxidation layer.

Methods. Polymer thin films were coated on silicon wafers using a P-6000 Spin Coater (Specialty Coating System, Inc.). Immediately before the coating, silicon wafers were rinsed with sufficient water, acetone, and toluene and subsequently spun at 2000 rpm to yield a smooth dry film. Polystyrene and poly(vinylphenol) were dissolved into toluene (Aldrich) and pyridine (Fisher Scientific), respectively, to give a final solution concentration of 1 wt %. The wafers were first covered with polystyrene or poly(vinylphenol) solutions and then spun at 2000 rpm. The spin acceleration was adjusted to be low enough to reduce the turbulent flow of the polymer solutions on the top of the wafers. Spun-cast polystyrene films were annealed under vacuum at 115 °C for 3 h and quenched to room temperature. Spun-cast poly(*p*-vinylphenol) films were an-

* Corresponding author. E-mail: peltonrh@mcmaster.ca.
† Department of Chemical Engineering, McMaster University.
‡ H. H. Wills Physics Laboratory, University of Bristol. E-mail: Robert.Richardson@bristol.ac.uk.
§ School of Chemistry, University of Bristol. E-mail: terence.cosgrove@bristol.ac.uk.
|| Department of Physics and Astronomy, McMaster University. E-mail: dalnoki@mcmaster.ca.
⊥ E-mail: luc2@mcmaster.ca.

10.1021/ma035130h CCC: $27.50
Published on Web 12/31/2003

nealed under vacuum at 140 °C for 16 h and quenched to room temperature. The integrity of the PS and PVPh films were confirmed using optical microscopy.

PS and PVPh films were also coated on a centimeter square silicon wafer using the same procedure mentioned above, and their surface roughnesses were measured using optical microscopy and atomic force microscopy. All the dry films gave a smooth surface with a root-mean-square roughness of around 3 Å.

The wafers were supported in the cell provided by NIST. In this configuration, the wafer is horizontal with the polymer coated side facing down into the aqueous solution. The neutron beam enters the side of the 1 cm thick wafer, reflects off the wafer/solution interfaces, and exits through the side of the wafer to enter the detector.

The 100 mg/L PEO solutions were mixed overnight before use. The wafer surfaces were equilibrated for an hour before data collection. Multiple runs showed no kinetic effects on the time scale of hours.

Neutron reflectivity measurements were performed on the NG-7 cold neutron reflectometer at the National Institute of Standards and Technology in Gaithersburg, MD. Neutrons of wavelength $\lambda = 4.75$ Å and energy resolution $\Delta\lambda/\lambda \approx 0.02$ were obtained from reflection of the white beam from a graphite monochromator. Reflectivity profiles were obtained by rotating the sample θ and detector 2θ degrees with reference to the incident beam, with a resolution $\Delta Q/Q \approx 0.04$. The reflected neutrons were detected using a simple ^{3}He detector. The detector counts were corrected for detector dead time. The incoherent background was measured by titling the sample away from the specular position, and this background was subtracted from the specular data.

The theoretical neutron reflectivity was calculated using Parratt32, version 1.5.0 (Berlin Neutron Scattering Center), and evaluated against the experimental data. Simultaneous fits of two data sets and fitting parameter sensitivity analyses were performed with software created by Robert Richardson. The polymer thin films were modeled to consist of adjacent layers of an assumed thickness d_i and an assumed scattering length density ρ_i. The interfaces between adjacent layers were characterized by a root-mean-square roughness σ_i, which describes the interface between layer $i - 1$ and i. During the fitting of reflectivity profile, model parameters d_i, ρ_i, and σ_i were varied iteratively until a good fit was achieved.

Results

In this work, neutron reflectivity was applied to study PEO adsorption at PS/water and PVPh/water interfaces. In a typical measurement, the intensity of the reflected neutron beam was recorded as a function of the scattering vector ($Q = 4\pi \sin\theta/\lambda$). Figure 1 shows the reflectivity profiles of a thin polystyrene film on a thick silicon wafer in contact with D_2O. The solid line is the fit of the reflectivity profile and the inset of Figure 1 shows the neutron scattering length density profile used to generate the fit. The horizontal axis of the inset corresponds to the distance (z) perpendicular to the polystyrene film. The data were fit with a three-layer model (silicon−polystyrene−D_2O) whose parameters are summarized in Table 1. The first layer is the bulk silicon wafer with a scattering length density of 2.07×10^{-6} Å^{-2}, the second layer is the thin H−PS film with a thickness of 492.4 Å and a scattering length density of 1.41×10^{-6} Å^{-1}, and the third layer is the bulk D_2O with a scattering length density of 6.37×10^{-6} Å^{-2}. The measured scattering length density of the PS film agrees with the theoretical scattering length density of pure PS, confirming that D_2O did not swell the PS film.

Figure 1 also shows the measured reflectivity profile of the same H−PS film under D_2O in the presence of H−PEO. The reflectivity profiles, with and without

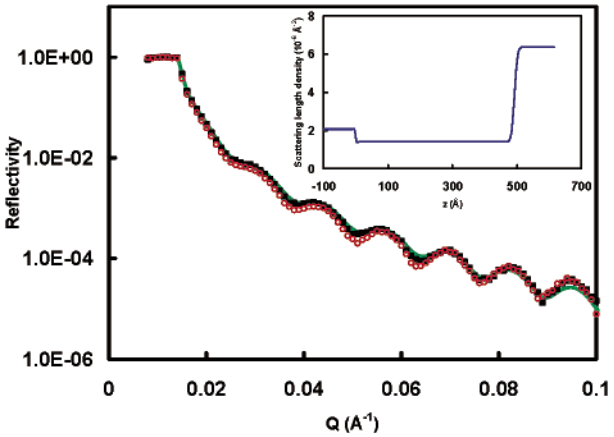

Figure 1. Neutron reflectivity profile and the fit for the H−PS film under D_2O with and without H−PEO at pH = 6.6. The circles represent the experimental data measured in the absence of H−PEO, the solid squares represent the experimental data measured in the presence of H−PEO, and the solid line represents the fit for the circles. The inset shows the scattering length density profile used to generate the fit.

Table 1. Parameters Used To Fit the Neutron Reflectivity Profile of the H−PS Film under D_2O at pH = 6.6

layer	composition (vol fraction)	thickness (Å)	ρ (10^{-6} Å^{-2})	roughness (Å)
1	Si	N/A	2.07	N/A
2	100% H−PS	492.4	1.41	0
3	D_2O	N/A	6.37	10

H−PEO, overlap, suggesting that H−PEO did not adsorb onto spin coated polystyrene surface.

Two coated H−PVPh films were used to study the interaction between PEO and PVPh surfaces. The structures of the two H−PVPh films were first studied under D_2O using neutron reflectivity, and the reflectivity profiles and the fitting parameters are shown in Figure 2 and Table 2. pH 6.6 was chosen since it is well below the pK_a value (9.9) of PVPh. At higher pH values, the PVPh film would become charged and water-soluble. The film PVPh1 had a thickness of 438 Å and a scattering length density of 2.76×10^{-6} Å^{-2}, and the film PVPh2 had a thickness of 434 Å and a scattering length density of 2.68×10^{-6} Å^{-2}. Since the measured scattering length densities of both films under D_2O were much larger than the theoretical scattering length densities of pure H−PVPh (1.74×10^{-6} Å^{-2}), we concluded that both H−PVPh films were swollen by D_2O. It is also well-known that deuterium can exchange with phenolic hydroxyl hydrogen in water. Therefore, the scattering length density of PVPh was recalculated to be 2.36×10^{-6} Å^{-2} by assuming all the phenolic hydroxyl hydrogen atoms in PVPh films were replaced by deuterium atoms. The fitting revealed that the D_2O volume fractions in the PVPh1 film and the PVPh2 film were 10.0% and 8.0%.

The properties of the PVPh films in the presence of PEO were determined by performing complementary experiments: D−PEO in D_2O (Figure 3); D−PEO in H2O (Figure 4); H−PEO in D_2O (Figure 5). Two approaches were used for fitting. In the first approach, individual data sets were fitted with Parratt32 and the results (see below) revealed that PEO sorption produced two new layers—an interpenetration layer in which PEO and PVPh formed a complex (blend) and a hydrated PEO corona layer facing the water. In the second fitting

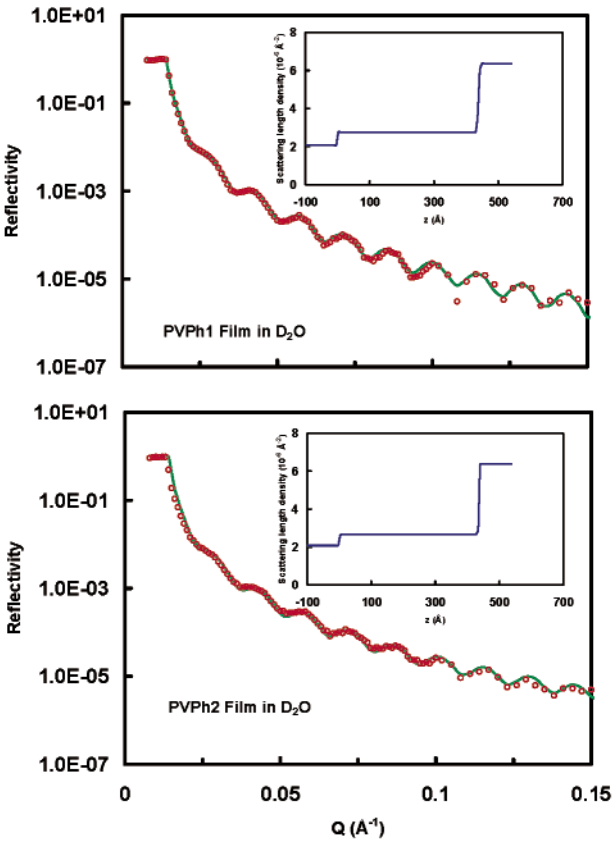

Figure 2. Neutron reflectivity profiles and fits for H−PVPh1 and H−PVPh2 films under D_2O at pH = 6.6. The circles represent the experimental data, and the solid lines represent the fits. The insets show the scattering length density profiles used to generate the fits.

Table 2. Parameters Used To Fit the Neutron Reflectivity Profiles of PVPh1 and PVPh2 Films under D_2O at pH = 6.6

layer	composition (vol fraction)	thickness (Å)	ρ (10^{-6} Å^{-2})	roughness (Å)
	PVPh1			
1	Si	N/A	2.07	N/A
2	90.0% H−PVPh, 10.0% D_2O	438.2	2.76	0
3	D_2O	N/A	6.37	5
	PVPh2			
1	Si	N/A	2.07	N/A
2	92.0% H−PVPh, 8.0% D_2O	434.0	2.68	2
3	D_2O	N/A	6.37	2

approach, complementary data sets were simultaneously fit, giving essentially the same results.

Figure 3 shows the reflectivity profile for the PVPh2 film under D_2O with and without D−PEO. Under these conditions, PEO in water is invisible to neutrons because the scattering length densities are nearly matched (D−PEO is 6.33×10^{-6} Å^{-2} and D_2O is 6.37×10^{-6} Å^{-2}). Thus, adsorbed PEO should not change the reflectivity profile providing the PEO does not penetrate or rearrange the poly(vinylphenol) film. Comparison of the reflectivity data, with and without D−PEO in Figure 3, shows clearly that the adsorption of D−PEO altered the reflectivity profile of the PVPh2 film. To fit the PEO data, it was necessary to include an additional thin layer between the PVPh film and the water (see Table 3 for parameters). This layer was assumed to be due to the interpenetration of PVPh gel (~10% water) with PEO. The modeling suggests that the thickness of the pure

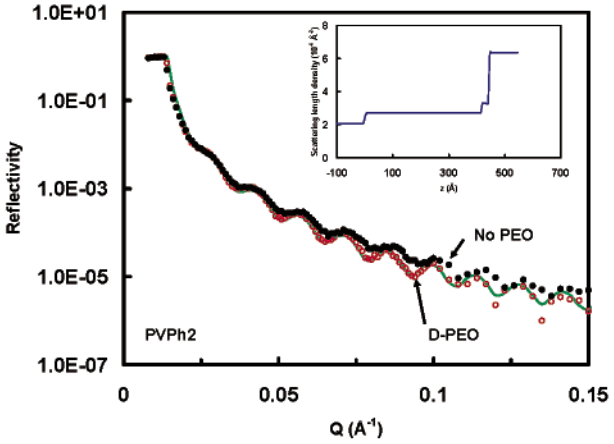

Figure 3. Neutron reflectivity profiles and the fit for the PVPh2 film under D_2O in the presence of D−PEO at pH = 6.6. The open circles represent the experimental data measured in the presence of D−PEO, and the solid line is the corresponding fit. The solid circles represent the experimental data measured without D−PEO. The inset shows the scattering length density profile used to generate the fit.

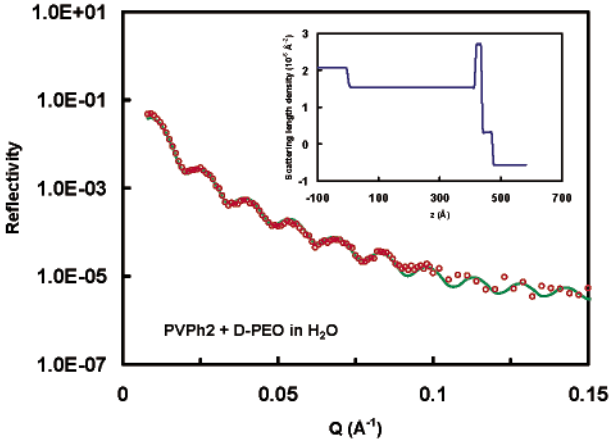

Figure 4. Neutron reflectivity profile and the fit for the PVPh2 film under H_2O in the presence of D−PEO at pH = 6.6. The circles represent the experimental reflectivity profile, and the solid line represents the fit for the circles. The inset shows the scattering length density profile used to generate the fit.

PVPh2 film was reduced by 19 Å corresponding to the interpenetration layer was 25 Å thick with a scattering length density of 3.32×10^{-6} Å^{-2}. Assuming the scattering length density of D_2O was the same as that of D−PEO, the volume fraction of H−PVPh in the interpenetration layer was calculated to be 76%.

To determine the volume fractions of D−PEO and water in the interpenetration layer and also the structure of the adsorbed PEO molecules on top of the interpenetration layer (the PEO corona layer), the reflectivity profile of the PVPh2 film in the presence of D−PEO was also measured under H_2O. The experimental profile and the fit are shown in Figure 4. During the fitting, the scattering length densities and the thicknesses of the PVPh2 film, the interpenetration layer and the PEO corona were varied iteratively to obtain a good fit. Table 4 shows the parameters used to generate the fit. The thickness of the interpenetration layer was 25 Å, close to the thickness shown in Figure 3. The volume fractions of D−PEO and H_2O in the interpenetration layer were estimated to be 22% and 2.3%.

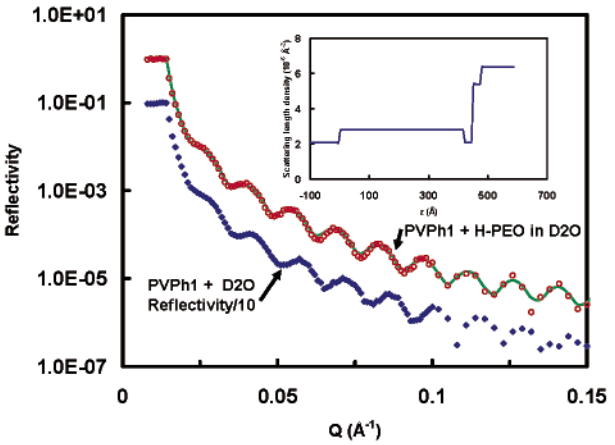

Figure 5. Neutron reflectivity profile and the fit for the PVPh1 film under D_2O in the presence of H−PEO at pH = 6.6. The circles represent the experimental reflectivity profile, and the solid line represents the fit for the circles. For comparison, the PVPh1 + D_2O curve from Figure 2A has been replotted with the reflectivity decreased by 10 for clarity. The inset shows the scattering length density profile used to generate the fit.

The corresponding adsorbed layer concentration, Γ (mg/m^2) was estimated to be 1.15 mg/m^2 based on the following equation

$$\Gamma = \rho_m(d_3\phi_{3-PEO} + d_4\phi_{4-PEO}) \quad (1)$$

where ρ_m is the mass density of pure PEO, d_3 and d_4 are the thicknesses of the interpenetration layer and the PEO corona, and ϕ_{3-PEO} and ϕ_{4-PEO} are the corresponding PEO volume fractions.

Since the parameters of the adsorbed PEO layer presented in Table 4 was determined by model fitting, it is possible that a different model might also give a good fit. To increase confidence in our proposed model, the neutron reflectivity profile of the H−PVPh film was also measured under D_2O in the presence of H−PEO. Figure 5 shows the experimental reflectivity profile and the fit, and Table 5 shows the parameters of a three-layer model used to generate the fit. The first layer was the PVPh1 film with a thickness of 422.6 Å and a D_2O volume fraction of 10.7%. The second layer corresponded to the interpenetration layer with a thickness of 26.0 Å and a scattering length density of 2.09×10^{-6} Å^{-2}. By assuming that the H−PVPh volume fraction was 75.8% obtained from Table 3, the volume fractions of H−PEO and D_2O were calculated to be 21.3% and 2.9%. The third layer corresponded to the H−PEO corona, and its thickness and the H−PEO volume fraction were fitted to be 26.9 Å and 16.7%. The specific adsorption amount of H−PEO on the PVPh1 film was estimated to be 1.25 mg/m^2.

In summary, the structure of the adsorbed PEO molecules (150 kDa) at the PVPh/water interface was studied at pH 6.6 using three different PEO/water mixtures: D−PEO/D_2O, D−PEO/H_2O, and H−PEO/D_2O. The fits of the experimental reflectivity profiles from all three mixtures gave nearly the same interfacial structure which is illustrated schematically in Figure 6. PEO penetrates 25.0 Å into the PVPh layer lowering the water content from 10.0% to 2.3% and the PVPh content from 90.0% to 75.8%. The remainder (∼45%) of the adsorbed PEO extends 30.9 Å into the aqueous phase with an average polymer volume fraction of 12.5% to give an overall PEO coverage of 1.2 mg/m^2. The correctness of this picture depends on the validity of the modeling. We have confirmed the uniqueness of this model by simultaneously fitting the same model to the reflectivity data from the PVPh/D−PEO/D_2O and the PVPh/D−PEO/H_2O samples. The scattering length densities of PVPh thin film (ρ_2), interpenetration layer (ρ_3), and PEO corona (ρ_4) were calculated as

$$\rho_2 = \rho_{PVPh}\phi_{2-PVPh} + \rho_w(1 - \phi_{2-PVPh}) \quad (2)$$

$$\rho_3 = \rho_{PVPh}\phi_{3-PVPh} + \rho_{PEO}\phi_{3-PEO} + \rho_w(1 - \phi_{3-PVPh} - \phi_{3-PEO}) \quad (3)$$

$$\rho_4 = \rho_{PEO}\phi_{4-PEO} + \rho_w(1 - \phi_{4-PEO}) \quad (4)$$

where ρ_{PVPh}, ρ_{PEO}, and ρ_w are the scattering length densities of PVPh, PEO, and water, ϕ_{2-PVPh} and ϕ_{3-PVPh} are the volume fractions of PVPh in the PVPh film and in the interpenetration layer, and ϕ_{3-PEO} amd ϕ_{4-PEO} are the volume fractions of PEO in the interpenetration layer and in the PEO corona. For the system containing H_2O, $\rho_{PVPh} = 1.73 \times 10^{-5}$Å^{-2} and $\rho_w = -0.55 \times 10^{-5}$Å^{-2} for H_2O. For the system containing D_2O, $\rho_{PVPh} = 2.34 \times 10^{-5}$Å^{-2}, assuming the hydroxyl proton was exchanged for a deuteron, and $\rho_w = 6.35 \times 10^{-5}$Å^{-2} for D_2O. The value of ϕ_{2-PVPh} was fixed at the value of 0.91 which was determined by the fit to the PVPh/D_2O reflectivity. The fit was then performed by allowing the volume fraction parameters, ϕ_{3-PVPh}, ϕ_{3-PEO}, and ϕ_{4-PEO}, and the layer thicknesses, d_2 (PVPh film), d_3 (interpenetration layer), and d_4 (PEO corona), to vary. Fits of similar quality to those obtained by fitting individual reflectivity (shown in Figures 3 and 4) profiles were obtained. The best fit parameters were very similar to those in Tables 3 and 4 confirming that they represent a self-consistent model of the surface structure.

The uniqueness of the model was then examined by exploring the goodness of fit χ^2 as pairs of parameters are stepped through a range of values near the best fit values. For each pair of the parameters being stepped, the remaining parameters were allowed to refine to give the best fit. The contour map of χ^2 as a function of the two parameters would show a single minimum if there is no correlation between the two parameters and an elongated valley if they were correlated. It was found that there was a strong inverse correlation between the volume fraction of PEO and the thickness of the layers. However, the product was constant indicating that the amount in the layers was reasonably well-defined, while the thicknesses of interpenetration layer and PEO corona layer were not. Parts A−D of Figure 7 show some results from the simultaneous fit described above. Figure 7A illustrates that the volume fraction of PVPh in the interpenetration layer (layer 3) is well-defined at $\phi_{3-PVPh} = 0.80 \pm 0.02$. The thickness of this layer is greater than about 30 Å. However, its maximum possible thickness is not well-defined by the data. Figure 7B shows that the volume fraction of PEO in interpenetration layer is also well-defined at 0.13 ± 0.03 but again the thickness is only roughly defined as 30 to 80 Å. Figure 7C shows that the two volume fractions, ϕ_{3-PVPh} and ϕ_{3-PEO} are correlated; however, there is a clear indication that $\phi_{3-PVPh} \sim 0.8$ and $\phi_{3-PEO} \sim 0.1$ is preferred. Figure 7D shows that the again the thickness is only roughly defined as 30−80 Å. The Figure 7C shows that two volume fractions, ϕ_{3-PEO} and ϕ_{4-PEO}, are weakly correlated with an indication that ϕ_{3-PEO} is in the range 0.1−0.2 and ϕ_{4-PEO} is less than 0.3. We are

Table 3. Parameters Used To Fit the Neutron Reflectivity Profile of the PVPh2 Film under D_2O in the Presence of D−PEO at pH = 6.6

layer	composition (vol fraction)	thickness (Å)	ρ (10^{-6} Å^{-2})	roughness (Å)
1	Si	N/A	2.07	N/A
2	91.2% H−PVPh, 8.8% D_2O	417.3	2.71	2
3	75.8% H−PVPh, 24.2% D-PEO and D_2O	25.4	3.32	0
4	D_2O	N/A	6.37	0

Table 4. Parameters Used To Fit the Neutron Reflectivity Profile of the PVPh2 Film under H_2O in the Presence of D−PEO at pH = 6.6

layer	composition (vol fraction)	thickness (Å)	ρ (10^{-6} Å^{-2})	roughness (Å)
1	Si	N/A	2.07	N/A
2	91.4% H−PVPh, 8.6% H_2O	417.0	1.54	3
3	75.8% H−PVPh, 21.8% D-PEO, and 2.4% H_2O	25.0	2.70	0
4	12.5% D-PEO, 87.5% H_2O	30.9	0.30	0
5	H_2O	N/A	−0.56	0

Table 5. Parameters Used to Fit the Neutron Reflectivity Profile of the PVPh1 Film under D_2O in the Presence of H−PEO at pH = 6.6

layer	composition (vol fraction)	thickness (Å)	ρ (10^{-6} Å^{-2})	roughness (Å)
1	Si	N/A	2.07	N/A
2	89.3% H−PVPh, 10.7% H_2O	422.6	2.79	0
3	75.8% H−PVPh, 21.3% H−PEO, and 2.9% D_2O	26.0	2.09	0
4	16.7% H−PEO, 83.3% D_2O	26.9	5.41	0
5	D_2O	N/A	6.37	0

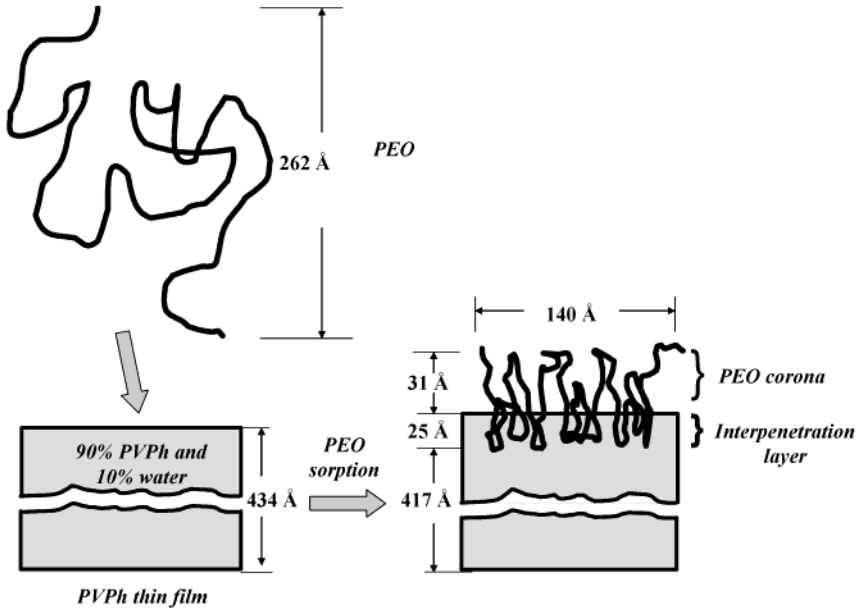

Figure 6. Schematic illustration of an adsorbed PEO molecule at the PVPh/water interface.

therefore confident that there was a layer at the surface of the PVPh film which contained PEO and a reduced volume fraction of PVPh relative to the rest of the film.

Discussion

We believe that this work is the first report of the structure of an adsorbed polymer truly penetrating the solid substrate. The behavior is a consequence of the attractive interactions between PEO and PVPh. In the solid state PEO forms completely miscible blends with PVPh due to hydrogen bonding between polyether oxygens and phenolic hydroxyls.[6,7] On the basis of melting point depression, Qin et al. estimated that the Flory−Huggins interaction parameter, χ_{12}, for the PEO−PVPh system is −1.5, indicating an exothermic interaction.[8] The presence of water in our experiments is an additional complication. We have studied the interaction of water-soluble PVPh copolymers with PEO in water, and not only is the main interaction hydrogen bonding but also it involves the PEO methylene groups sitting on or between the π orbitals of the aromatic ring.[9]

In this work the strong PEO/PVPh interactions lead to significant adsorption and penetration of PEO into the PVPh layer. It is instructive to compare the measured adsorption amounts with the predicted values on hard surfaces. The hydrodynamic radius R_h of the aqueous D−PEO (M = 150 kDa) was estimated to be 131 Å from the equation proposed by Devanand et al. ($R_h = 0.145M^{0.571}$ Å).[10] If the PEO molecules are considered to be spheres with radius equal to R_h which have cubic packing on a planar surface, the corresponding surface coverage should be 0.35 mg/m^2, which is

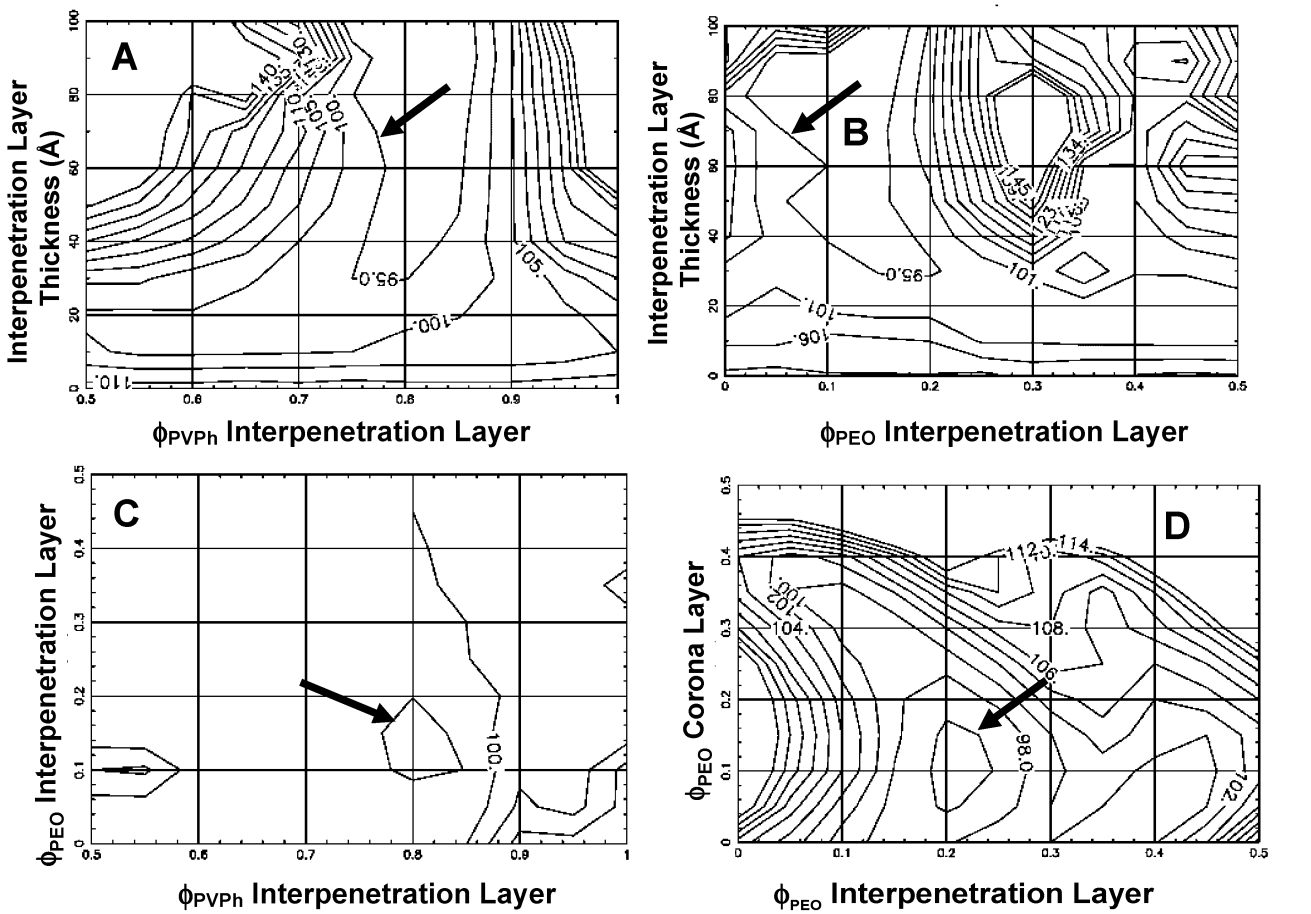

Figure 7. Contours of constant χ_2 for the fits as functions of adjustable variables. The arrow indicates the best fit regime (i.e., the lowest $\chi 2$ contour).

around one-fourth of the observed value. Also, the combined thickness of the PEO interpenetration layer and the PEO surface layer was about 50 Å, which is one-fifth of the PEO hydrodynamic diameter. Thus, the PEO molecules adsorbed onto the PVPh films are much more compact than the free PEO molecules in solution.

We propose that PEO adsorption onto PVPh is more correctly considered to be "absorption" and the driving force is polymer/polymer complex formation. Furthermore, like many of the instances where PEO binds to water-soluble phenolics, complex formation is accompanied by a deswelling and collapse of the PEO coil.[11,12] It seems reasonable to propose that the PEO chains are kinetically arrested and that our results portray a "snapshot" of a polymer entering a solid phase.

Finally, our inability to detect PEO adsorption onto polystyrene was in accordance with the earlier work of Cosgrove and co-workers who showed that PEO chains terminally grafted to polystyrene latex do not adsorb on hydrophobic, low charge density polystyrene latex[13] whereas many workers have shown that PEO readily adsorbs onto conventional, persulfate initiated surfactant-free PS latex surfaces.[14] We speculate that carboxyl groups, usually present in persulfate-initiated latexes, may drive PEO adsorption in these systems. Thus, the polystyrene films used in this work were simply too pristine and thus too hydrophobic for PEO adsorption.

Conclusions

In summary, we have been able to measure the penetration of PEO into slightly water-swollen PVPh thin films giving an embedded surface PEO layer with a PEO concentration of 1 to 2 mg/m^2. This is at least three times greater than the estimated value for close packing of PEO coils on a flat impenetrable surface. The reflectivity data could be fitted by a multilayer model in which about half of each sorbed PEO molecule is inside the PVPh film and the remainder is on the surface. We propose that this surface architecture is fundamentally different than either PEO adsorbed or grafted to hard surfaces. Furthermore, such surfaces may provide an alternative strategy to grafting and to block copolymer adsorption for preparation of PEO-rich surfaces for biocompatible materials.

Acknowledgment. This work was supported by ONDEO-Nalco Co. and the Canadian Government NSERC-CRD program. We acknowledge the help of Sushil Satija from NIST and support of the National Institute of Standards and Technology, U.S. Department of Commerce, in providing the neutron research facilities used in this work.

References and Notes

(1) Fleer, G. J.; Cohen Stuart, M. A.; Scheutjens, J. M. H.; Cosgrove, T.; Vincent, B. *Polymers at Interfaces*; Chapman & Hall: London, 1993.

(2) Coleman, M. M.; Graf, J. F.; Painter, P. C.; *Specific Interactions and the Miscibility of Polymer Blends*; Technomic: Lancaster, PA, 1991.

(3) Harris, J. M. *Poly(ethylene glycol) Chemistry: Biotechnical and Biomedical Applications*; Plenum Press: New York, 1992.

(4) Fragneto-Cusani, G. *J. Phys.: Condens. Matter* **2001**, *13*, 4973−4989.
(5) Penfold, J.; Thomas, R. K. *J. Phys.: Condens. Matter* **1990**, *2*, 1369−1412.
(6) Coleman, M. M.; Graf, J. F.; Painter, P. C.; *Specific Interactions and the Miscibility of Polymer Blends*; Technomic: Lancaster, PA, 1991.
(7) Moskala, E. J.; Varnell, D. F.; Coleman, M. M. *Polymer* **1885**, *26*, 288.
(8) Qin, C.; Pires, A. T. N.; Belfiore, L. A. *Polym. Commun.* **1990**, *31*, 177.
(9) Cong, R.; Bain, A. D.; Pelton, R. H. *J. Polym. Sci. B* **2000**, *38*, 1276.
(10) Devanand, K.; Selser, J. C. *Macromolecules* **1991**, *24*, 5943.
(11) Stack, K. R.; Dunn, L. A.; Robert, N. K. *J. Wood Chem. Technol.* **1993**, *13*, 283.
(12) Lu, C.; Pelton, R. *Supermolecular Structure of PEO/Tyrosine-containing Polypeptide Aqueous Complexes*, to be submitted for publication.
(13) Cosgrove, T.; Heath, T. G.; Ryan, K.; van Lent, B. *Polym. Commun.* **1987**, *28*, 64.
(14) Pelssers, E. G. M.; Cohen Stuart, M. A.; Fleer, G. J. *Colloids Surf.* **1989**, *38*, 15. (b) Pelssers, E. G. M.; Cohen Stuart, M. A.; Fleer, G. J. *J. Chem. Soc., Faraday Trans.* **1990**, *86*, 1355.

MA035130H